

Received: 2016.02.21
Accepted: 2016.04.11
Published: 2016.11.29

Effect of Bone Marrow Mesenchymal Stem Cells on Satellite Cell Proliferation and Apoptosis in Immobilization-Induced Muscle Atrophy in Rats

Authors' Contribution:
Study Design A
Data Collection B
Statistical Analysis C
Data Interpretation D
Manuscript Preparation E
Literature Search F
Funds Collection G

A 1,2 **Tie-Shan Li**
B 3 **Hao Shi**
C 2 **Lin Wang**
AD 1,4 **Chuan-Zhu Yan**

1 Department of Neurology and Neuromuscular Center, Qilu Hospital of Shandong University, Jinan, Shandong, P.R. China
2 Department of Rehabilitation, The Affiliated Hospital of Qingdao University, Qingdao, Shandong, P.R. China
3 Shandong Rehabilitation Research Center, Jinan, Shandong, P.R. China
4 Brain Science Research Institute, Shandong University, Jinan, Shandong, P.R. China

Corresponding Author: Changzhou Yan, e-mail: chuanzhuyan@163.com
Source of support: Departmental sources

Background: Muscle atrophy due to disuse occurs along with adverse physiological and functional changes, but bone marrow stromal cells (MSCs) may be able to act as muscle satellite cells to restore myofibers. Thus, we investigated whether MSCs could enhance the proliferation of satellite cells and suppress myonuclear apoptosis during immobilization.


Material/Methods: We isolated, purified, amplified, and identified MSCs. Rats (n=48) were randomized into 3 groups: WB group (n=16), IM-PBS group (n=16), and IM-MSC (n=16). Rat hind limbs were immobilized for 14 d, treated with MSCs or phosphate-buffered saline (PBS), and then studied using immunohistochemistry and Western blot analysis to characterize the proteins involved. Apoptosis was assessed by terminal deoxynucleotidyl transferase (TdT)-mediated deoxy-UTP nick end labeling (TUNEL) method.

Results: We compared muscle mass, cross-sectional areas, and peak tetanic forces and noted insignificant differences between PBS- and MSC-treated animals, but satellite cell proliferation was significantly greater after MSC treatment (p<0.05). Apoptotic myonuclei were reduced (p<0.05) after MSC treatment as well. Pro-apoptotic Bax was down-regulated and anti-apoptotic Bcl-2 and p-Akt protein were upregulated (p<0.05).

Conclusions: MSCs injected during hind limb immobilization can maintain satellite cell activity by suppressing myonuclear apoptosis.

MeSH Keywords: **Apoptosis • bcl-2-Associated X Protein • Immobilization • Mesenchymal Stromal Cells • Muscular Atrophy • Satellite Cells, Skeletal Muscle**

Full-text PDF: <http://www.medscimonit.com/abstract/index/idArt/898137>

 3407

 1

 6

 30



1 Background

Skeletal muscle, which accounts for about 40% of the human body mass, is necessary for motion and optimal health.

5 Decreased muscle mass can reduce quality of life and impair health. Skeletal muscle phenotypes change depending on the mechanical load placed upon them. For instance, increased mechanical load stimulates hypertrophy, whereas an absence of mechanical load (or a normal gravitational load) causes muscle atrophy; this can be seen in astronauts during adaptation to hypogravity. Muscle disuse includes reduced mechanical load or the mechanical unloading of muscle, and both cause decreased volume of existing skeletal muscle myofibers, which is manifested as reduced muscle size or "disuse atrophy." Such atrophy
10 occurs after bone or CNS injury [1,2], prolonged disease states, or neurological illnesses [3]. Human models of disuse, such as deliberate or injury-mediated immobilization, as well as sedentary lifestyles (inactivity), feature decreased mechanical loading. This eventually causes muscle wasting and weakening and
15 subsequent metabolic consequences that affect overall health.

Muscles that must work against gravity, such as the soleus, gastrocnemius, and vastus lateralis, are most commonly adversely affected by immobilization [4]. Their fibers undergo
20 apoptosis during atrophy, especially the soleus, which primarily consists of slow-twitch fibers. The soleus responds rapidly to disuse and can undergo fiber-type switching. Generalized skeletal muscle atrophy involves decreased protein production and cross-sectional area (CSA), which contribute to
25 reduced force production.

PI3K/Akt/mTOR is a crucial signaling pathway that increases protein synthesis [5] and muscle mass recovery after immobilization; it depends on generation of a sustained positive
30 nitrogen balance due to normalization of changes in protein metabolism associated with increased protein synthesis. Akt phosphorylation is sufficient for dramatic muscle hypertrophy and inhibition of atrophy [6,7]. Simultaneously, apoptosis is generally regulated by complex proteins such as pro-apoptosis (Bax) and anti-apoptosis (Bcl-2) proteins. The balance between Bax and Bcl-2 determines whether a cell will undergo
35 apoptosis or survive.

Satellite cells were reduced during immobilization periods after disuse, perhaps caused by impaired proliferation. Because adult myofibers are terminally differentiated, the regeneration of skeletal muscle is largely dependent on a small population of satellite cells, which are located between the sarcolemma and the basal lamina of the muscle fiber. Satellite cells are
40 responsible for providing myonuclei for postnatal growth or repair [8,9]. After muscle injury, satellite cells become activated and divide, forming new myofibers or repairing existing fibers. Previously, satellite cells were thought to be optimal for
45

transplant into injured or dystrophic skeletal muscles. However, many studies indicated that satellite cells have limited utility as donor cells [10]. First, the self-renewal potential of adult satellite cells is limited, decreases with age, and can be exhausted by a chronic regenerative processes such as severe
5 muscular dystrophy, in which most muscle tissue is eventually lost and is replaced by connective tissue. Secondly, satellite cells transplanted into damaged skeletal muscle have restricted migration and these cells readily undergo apoptosis. *In vitro* culture of satellite cell-derived myoblasts to expand populations causes loss of their regenerative ability [11].
10

Bone marrow stromal cells (MSCs) were reported to contribute to satellite cell function in cardiotoxin-injured muscle [12]. MSCs are under consideration for regenerative medicine as they
15 are easy to isolate and can be rapidly expanded from patients. After muscle injury, or for individuals with chronic degenerative myopathies, satellite cells divide and fuse to repair or replace damaged fibers. Research indicates that MSCs transplantation have therapeutic potential in animal experiments [13].
20 Indeed, MSCs has been confirmed to contribute to myofiber formation and to functional recovery of muscle tissue [14]. However, the effect of MSCs on muscle atrophy induced by immobilization is not clear. We hypothesized that the recovery of atrophic muscle induced by immobilization is due to increased satellite cell proliferation and inhibition of apoptosis.
25

Material and Methods

Isolation and culture of MSCs

MSCs were generated from bone marrow aspirates of normal male Wistar rats (80–100 g). Briefly, 5 rats were anesthetized for surgery and femur and tibial whole marrow was removed
35 and cleaned of all connective tissue. MSCs were cultured in a-modified DMEM with low glucose (HyClone Laboratories Logan, UT) supplemented with 10% FBS (HyClone Laboratories Logan, UT), 100 U/ml penicillin, and 100 mg/ml streptomycin (Gibco, Invitrogen, Carlsbad, CA) and incubated at 37°C in a
40 5% CO₂ humidified incubator (Thermo Fisher Scientific Japan, Yokohama, Japan). After 48 h, non-adherent cells were removed, fresh medium was added, and medium was changed weekly. When adherent cells were 90% confluent, they were trypsinized (0.25% trypsin and 0.02% EDTA; Invitrogen-Gibco Carlsbad, CA) and seeded onto fresh plates (split 1:3) until a homogeneous population was obtained after 2 to 3 weeks of culture. All experiments were performed using cells at 3–5 passages.
45

Cell-surface analysis and flow cytometry

Cells were seeded into 12-well culture plates and culture slides. When cultures reached 80–90% confluence, MSCs were fixed
53

1 with 4% paraformaldehyde for 40 min and were washed with PBS. FITC-conjugated antibodies (1:500, Sigma, St. Louis, MO) against rat CD34 or CD44, and phycoerythrin (PE)-conjugated antibodies (1:200, Invitrogen, Carlsbad, CA) against rat CD45
5 or CD90 (BD Pharmingen, San Diego, CA) were added to wells in the dark. After 60 min, MSCs seeded into 12-well culture plates were washed with PBS and harvested with 0.25% trypsin (Invitrogen, Carlsbad, CA) for 3 min at 37°C. Samples were then centrifuged and supernatant was removed and resuspended in
10 500 ml of HBS. Simultaneously, the control cells attached no antibody. Finally, cells were measured with flow cytometry and analyzed with Facs Canto II (Becton Dickinson and Company, Franklin Lakes, NJ) and the Facs DiVa software program.

15 Lentiviral transduction of MSC

Self-inactivating lentivirus expressing enhanced green fluorescent protein (GFP) cDNA under control of the β -actin/cytomegalovirus (CMV)/ β -globin intron hybrid promoter (LV-GFP)
20 was used [15]. Briefly, MSC were seeded at a density of 5×10^4 cells/well in 6-well plates and exposed to lentivirus for 24 h at 37°C with a multiplicity of infection (MOI) of 50. Virus-containing medium was removed and MSC were cultured for another 48 h in standard medium. GFP-expressing MSC were
25 selected by DiVa cell sorting (BD Biosciences, Heidelberg, Germany) and characterized as described above.

Animal immobilization with plaster casts

30 Male 3-month-old Wistar rats were obtained from the Experimental Animal Center of Qingdao Institute for Drug Control (Qingdao, China). The animals were housed under standard laboratory conditions at a stable temperature (22–24°C) and a 12-h light/dark cycle. This study was carried out
35 in strict accordance with the recommendations of National Institute of Health for the care of laboratory animals. The protocol was approved by the Committee on the Ethics of Animal Experiments of Qingdao University.

40 Rats (n=48) were randomized into 3 groups: WB (n=16) received no treatment except plaster casts; IM-PBS (n=16) were immobilized and received vehicle pbs; and IM-MSC (n=16) were immobilized and received MSCs. Modified plastic casts were applied as described previously [16]. First, rats were anesthetized
45 with 8% chloral hydrate (400 mg/kg, i.p.). Plaster casts were cut to 1.5-cm widths and 20–25 cm lengths and these were used to immobilize the right hind limb from the thigh to the foot, resulting in immobilization of the knee in the extension position and the ankle in the plantar flexion position. Sham-immobilized animals were immobilized such that the knee and ankle could move without restraint and this ensured that the approximately equal plaster casts were appended to the right
50 hind limb of each rat. The animals were immobilized for 14 d.

Transplantation of BM-MSCs in Rats

After 3–5 passages, LV-GFP-MSCs were detached with trypsin/EDTA, washed, and resuspended in PBS (final concentration 20
5 000 cells/ml) for transplantation. Plaster casts were removed after 24 h. MSCs (1×10^6 in PBS 50 ml) were injected into soleus in fixed limbs and this was the IM-MSC treatment group. The same volume of PBS without MSCs was given to controls (IM-PBS treatment group). Then, all animals were immobilized with the previously described methods.
10

Soleus histology

For routine histopathology, tissues were formalin-fixed, paraffin-embedded, and transverse soleus sections were cut (3- μ m
15 thickness) and stained with hematoxylin and eosin (H&E). Slides were evaluated under light microscopy, and microphotographs were taken with a digital camera (Leica, DM2500, Germany) attached to a microscope (Leica). Digitally captured images were processed and analyzed using ImageJ software.
20 Myofibers with centrally located nuclei were considered to be regenerating after injury. We randomly selected 100 regenerating myofibers and measured cross-sectional areas (CSA) using ImageJ software.
25

Force measurement

After 14 d of immobilization, rats were anesthetized with 8% chloral hydrate (400 mg/kg, i.p.). Soleus were surgically excised, and both ends of the dissected muscle were tied firmly with
30 non-absorbable black surgical silk. Muscles were weighed and mounted on an experimental chamber with a vertical organ bath containing mammalian Ringer's solution (22–24°C) bubbled with 95% O₂/5% CO₂. The solution included the following composition (in mM): NaCl 136, KCl 5, CaCl₂ 1.8, MgCl₂ 0.5,
35 NaHCO₃ 15, and NaH₂PO 1. Relationships of force-length, force-frequency, and peak tetanic force (Po) were established. This protocol has been previously described in detail [17]. The force-frequency relationship was established by stimulating the muscle at frequencies of 10, 20, 40, 60, 80, and 100 Hz. Immediately
40 following force mechanics, muscle weights were measured.

Western blot

Soleus were removed under sterile conditions for Western blot
45 analysis [18]. Briefly, muscles were homogenized in lysis buffer and protease inhibitors. Protein (20 μ g) was separated with 12% SDS-PAGE and transferred onto PVDF membranes (300 mA, 120 min). After overnight blocking with 5% non-fat milk in PBS containing 0.05% Tween 20 at 4°C, membranes were incubated
50 with primary antibodies for Phospho-Akt^{Ser473} (1:1000, #9271, Cell Signaling Technology, Danvers, MA), Akt (1:1000, #9272 Cell Signaling Technology), Bcl-2 (1:1000, G9545, Sigma-Aldrich), and
53

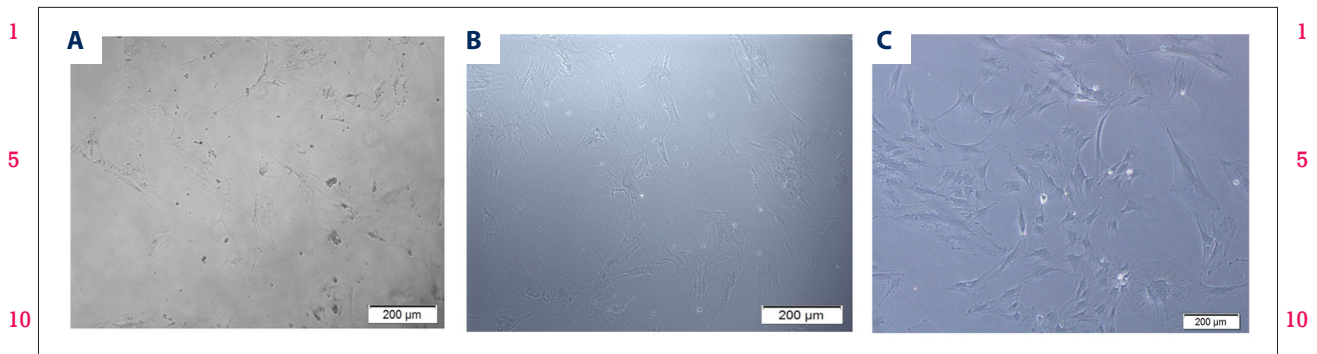


Figure 1. Morphology of MSCs. (A) Cells were mixed with non-adherent cells (200×). (B) Cells were spindle-shaped after the first change (200×). (C) Attached cells formed typical spindle shapes (200×).

15 Bax (1: 1000, B3428, Sigma-Aldrich) overnight at 4°C. Blots were also probed with anti-GAPDH monoclonal antibody (1:1000, G9545, Sigma-Aldrich) as a loading control. Subsequently, membranes were incubated in appropriate dilutions of goat anti-rabbit IgG H&L (HRP) secondary antibodies (1:10 000, ab97051, Abcam) diluted in 5% non-fat milk. Immunoreactive bands were detected using the BioSpectrum Imaging 810 System (UVP, Upland, CA) and quantified with ImageJ software.

BrdU incorporation and measurement

25 Animals were given water with BrdU (0.8 mg/ml) (Sigma, Saint Louis, MO) for 3 days after injection and then animals were sacrificed and soleus were removed 14 d after immobilization. Muscles were fixed and incubated with 2 N HCl for 20 min. 30 Samples were washed and sections were incubated with anti-BrdU (1:200; Sigma, Saint Louis, MO) and anti-Pax7 (1:200, Abcam) at 4°C overnight, followed by Alexa 594-conjugated goat anti-mouse IgG (1:500, Abcam) and Alexa 488-conjugated goat anti-rabbit IgG (1:500, Abcam). Finally, the sections 35 were incubated with DAPI (Life Technologies, Japan) for 1 min, washed in PBS, and mounted in mounting solution (Thermo Fisher Scientific). Positive cells were counted under 20 high-power fields (HPFs) of 25 sections and the relative number of Pax7/BrdU-positive cells in HPF was noted.

TUNEL staining

40 Apoptosis was assessed by use of a terminal deoxynucleotidyl transferase (TdT)- mediated deoxy-UTP nick end labeling (TUNEL) kit (Roche Applied Science, Indianapolis, IN). Six-micron-thick sections were cut and positioned on poly-lysine coated glass slides for 20 min and incubated with TUNEL reaction mixture (freshly prepared) for 60 min at 37°C in the dark. Nuclei were counterstained with DAPI. Sections were visualized under a fluorescence microscope (Eclipse 80i; Nikon, Tokyo, Japan). The photographs were analyzed using a graphics program (Image J) and the percentage of apoptotic positive cells per slide was calculated.

Statistical analysis

Statistical analysis was conducted using GraphPad Prism software (GraphPad Software Inc., USA). Statistical comparisons were made using the *t* test and one-way analysis of variance (ANOVA). Differences were considered statistically significant at a value of $P < 0.05$. All results are expressed as means \pm SEM of the indicated number of experiments and represent at least 3 independent experiments.

Results

Morphological characteristics of MSCs and flow cytometry analysis

30 In primary culture, MSCs were mixed with non-adherent cells (Figure 1A); however, following 2–3 passages, the cells were eliminated from the population (Figure 1B, 1C). MSCs contained 2 morphologically distinct cell types: spindle-shaped cells and large, flat cells. The specific surface antigen markers of MSCs were detected via immunofluorescence. The results of immunofluorescence staining demonstrated that the MSCs expressed CD44 and CD90. However, the expression of CD34 and CD45 was negative (Figure 2A).

40 The cells were analyzed for expression of MSCs markers using flow cytometry. The percentage of cells expressing the MSCs markers CD44, CD90, CD34, and CD45 are shown in Figure 2B. The percentages of CD44⁺, CD90⁺, CD34⁺, and CD45⁺ cells were calculated to be 93.83%, 96.88%, 6.32%, and 8.32%, respectively.

MSCs transplantation has no effect on soleus muscle mass, and cross-sectional area

50 Body weight showed no difference among groups (WB, IM-PBS, and IM-MS-C) at the start of the experiment or at the end of the 14-d immobilization period (Table 1). Soleus mass was normalized to body weight for comparisons. Soleus wet masses 53

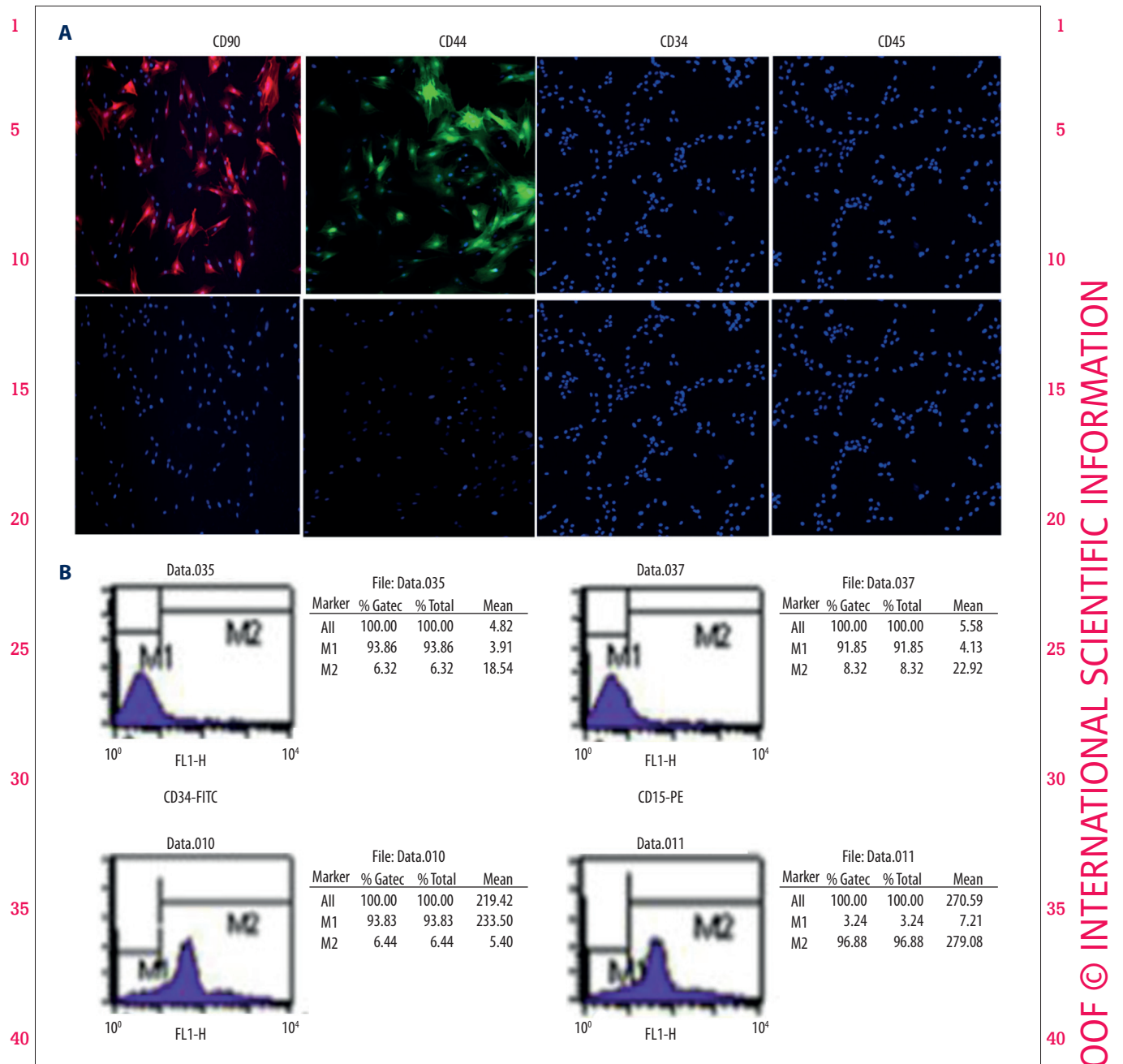
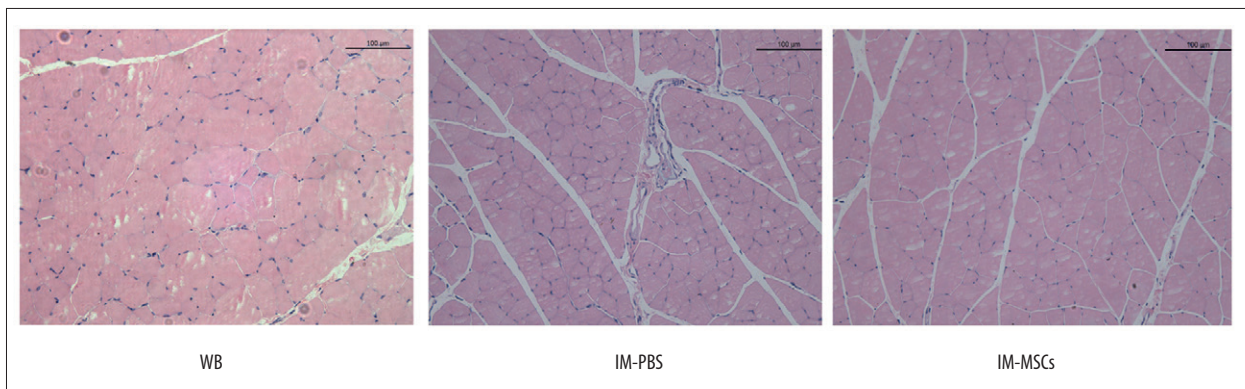


Figure 2. Specific surface markers of MSCs detected by immunofluorescence and flow cytometry analysis. **(A).** Immunofluorescence stained MSCs showing the specific surface markers of MSCs. The upper panel represents PE-CD90 (red), FITC-44 (green), FITC-34, and PE-45 counterstained with DAPI (blue) for nuclei identification. The lower panel represents DAPI (blue) for nuclei visualization. Immunofluorescence staining demonstrated that the MSCs expressed CD44 and CD90. However, the expression of CD34 and CD45 was negative. **(B).** MSCs were incubated with FITC-34, PE-45, FITC-44, and PE-CD90 antibody compared with control. The percentages of CD44⁺, CD90⁺, CD34⁺, and CD45⁺ cells were calculated to be 93.83%, 96.88%, 6.32%, and 8.32%, respectively.

1 **Table 1.** Body weight and muscle mass. 1

	N	Body weight (g)		Muscle mass (mg)	Normalized muscle mass (mg/g)
		Day 0	Day 14		
WB	16	252.37±1.14	268.56±1.81	187.10±1.12	0.70±0.67
IM-PBS	16	256.49±2.11	259.87±1.45	145.67±1.48*	0.55±0.81*
IM-MSCs	16	254.62±0.78	261.13±2.40	150.25±0.78*	0.57±0.33*

10 Body weight (BW), soleus muscle mass, and normalized muscle mass in WB, PBS, and MSC groups. * p<0.05, significant difference 10
compared to WB group. Values are means ±SEM.



25 **Figure 3.** Histology of soleus muscle and measurements of the cross-sectional area (CSA). 25

in the IM-PBS group were reduced compared with wet masses in the WB group (p<0.001; Table 1). MSCs improved muscle mass compared to WB controls but compared with PBS-treated animals, MSCs (IM-MSC group) did not stop the decrease in muscle mass. Mean muscle fiber cross-sectional solei areas in the IM-PBS group were significantly reduced compared with the WB group, and differences between IM-PBS and IM-MSC groups were significant (Table 1, Figure 3).

35 **Contractile properties of the soleus**

After normalizing Po to the cross-sectional area, IM-PBS Po was reduced compared with the WB group (p<0.05) but no significant difference was noted between IM-PBS and IM-MSC groups (date not shown).

Satellite cell proliferation

45 To detect changes in total satellite pools and proliferation after hind limb immobilization, we measured Pax7-immunoreactive nuclei and co-labeled them with BrdU (Figure 4A). Total satellite cells as indicated by Pax7 nuclei decreased by about half after 14 d of hind limb immobilization. Satellite cell proliferation was also reduced after hind limb immobilization. Measurements of BrdU⁺/Pax7⁺ double-positive nuclei among Pax7-immunoreactive cells indicated that MSCs not only prevented satellite cell decline but also significantly induced 53

satellite cell proliferation (p<0.05; Figure 4B). Compared with the IM-PBS group, the ratio of BrdU⁺/Pax7⁺ nuclei within the total Pax7⁺ population in the IM-MSC group was increased and was greater than that of the WB group (p<0.05; Figure 4B). 30

MSCs transplantation suppresses apoptosis

TUNEL was used to visualize DNA fragmentation to identify apoptotic myonuclei (Figure 5A), and apoptotic indices, represented by total apoptotic myonuclei per 10³ myofibers in solei, were significantly increased (p<0.05; Figure 5B) in the IM-PBS group compared with WB controls. MSCs significantly reduced apoptotic indices in the IM-MSC group compared with the IM-PBS group but the index was greater than in WB controls (p<0.05; Figure 5B).

MSCs activate the Akt pathway and regulate the expression of Bcl-2 and Bax

Insulin-like growth factor-1 (IGF-1)/phosphatidylinositol 3-kinase (PI3K)/Akt/mTOR is an important signaling pathway that increases protein synthesis, and Bax and Bcl-2 play important roles in regulation of the mitochondrial pathway of apoptosis. We assessed the expression of these proteins in soleus after 50 immobilization and investigated whether MSCs could change expression of these proteins. Western blot analysis indicated that in the IM-PBS group, Bax expression was higher (p<0.05; 53

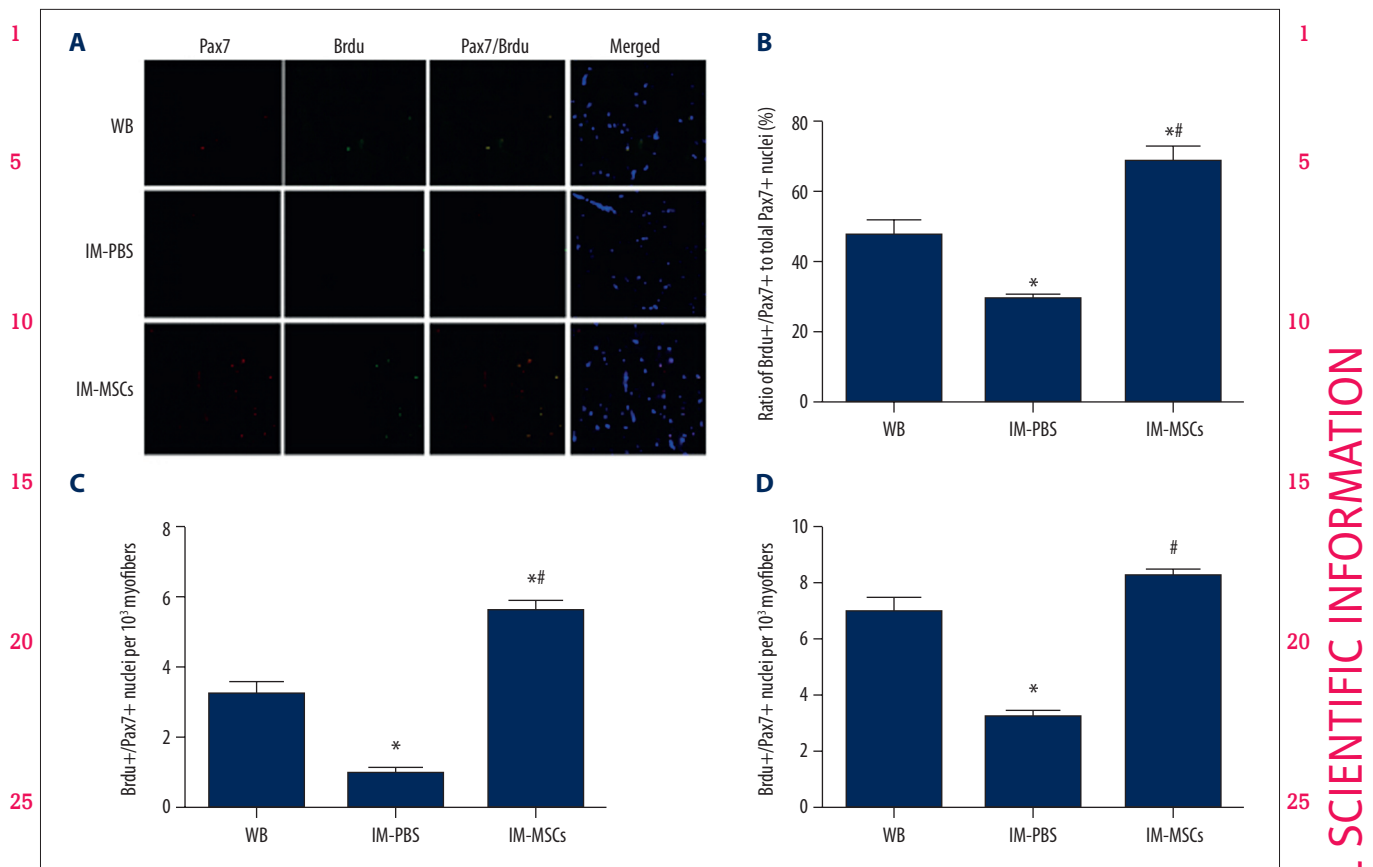


Figure 4. Satellite cell proliferation. (A) Immunohistochemistry of soleus cross-sections from all groups: Pax7 (red) and BrdU (green) expression, and nuclear (DAPI blue) identification. Yellow staining represents Pax7 and BrdU double-positive nuclei. Scale bar=25 mm. (B) Ratio of BrdU+/Pax7+ nuclei within the total Pax7+ population. (C) BrdU+/Pax7+ double-positive nuclei per 10³ myofibers. (D) Total Pax7 immunoreactive nuclei. * p<0.05, vs. WB group; # p<0.05, vs. IM-PBS group. The data presented are the mean ± standard deviation.

Figure 6A, 6C), and after MSC treatment Bax was reduced in the IM-MSC group compared with the IM-PBS group (p<0.05; Figure 6A, 6C). Bcl-2 (p<0.05; Figure 6A, 6B) and p-Akt (p<0.05; Figure 6A, 6D) expression was greater in the IM-PBS group and Bcl-2 expression was the greatest in the WB group, and the WB group had the least Bax expression (p<0.05; Figure 6A–6C).

Discussion

MSCs are accessible, have low immunogenicity and high multipotentiality, and they have been studied for muscle regeneration. Previous studies confirmed MSCs myogenic differentiation [19] and their potential for treating skeletal muscle diseases, but external factors are required [20]. When MSCs were transplanted into non-injured muscles, they remained undifferentiated, neither proliferating nor differentiating into mesenchymal cells, such as muscles and/or blood vessels (data not shown). Kuraitis [21] reported that myogenesis of MSCs *in vivo* required an extracellular matrix such as collagen

and severely stressed conditions such as an injury. We noted that immobilization with a plaster cast provided the requisite stress, and MSCs transplanted 24 h after injury had the greatest potential for muscle fiber differentiation from MSCs. Therefore, transplantation 24 h after immobilization was selected as a treatment time.

The results revealed a significant decrease in soleus mass in the IM-PBS group compared with the WB group, which is similar to published data [22]. However, there was no difference between the IM-PBS and IM-MSC groups in muscle mass or cross-sectional area, so MSCs did not improve these aspects. MSCs-induced changes were assessed by measuring changes in soleus contractile properties (Po, length-tension relationships, and force-frequency relationships). The present study demonstrated that Po was reduced and peak length-tension relationships were generated at shorter muscle lengths after muscle unloading. The reason for this may be sarcomere loss [23]. No significant difference was noted between IM-PBS and IM-MSC groups. Continuous immobilization for 14 d may

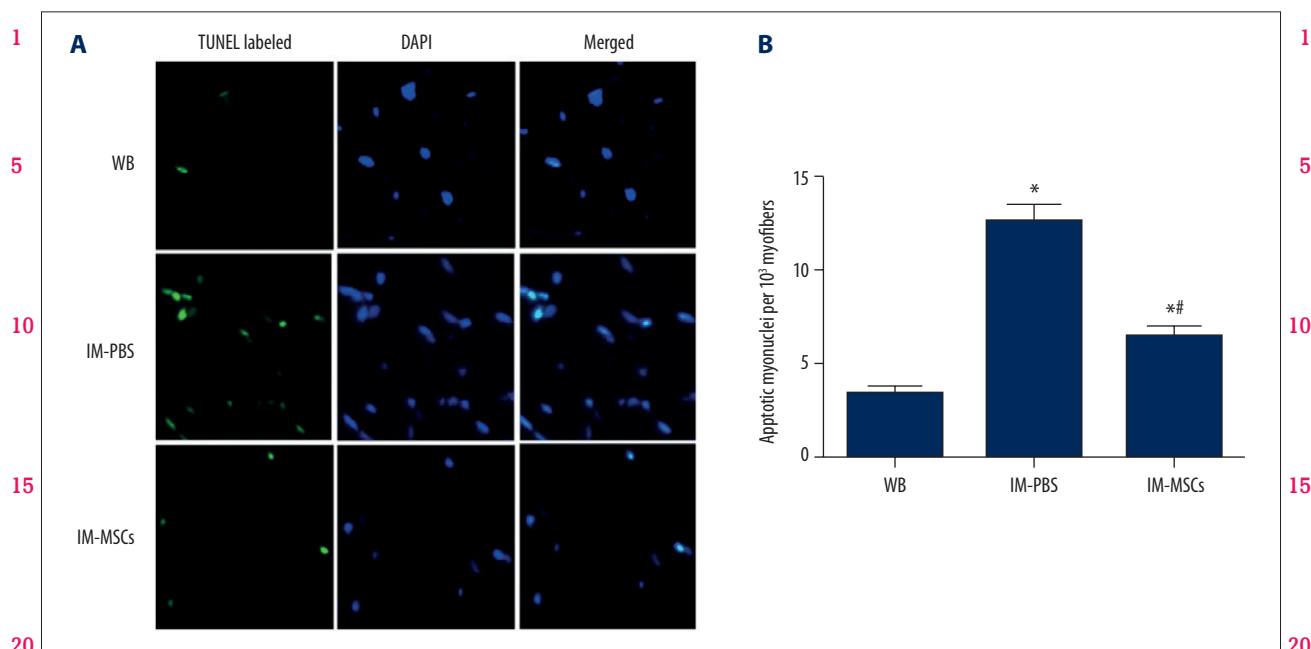


Figure 5. TUNEL analysis of soleus myofibers. **(A)** Representative TUNEL labeled (green) and DAPI-counterstained (blue) images indicate CSAs from weight-bearing (WB) animals, and those immobilized and then treated with PBS (IM-PBS), as well as those that were immobilized and then treated with MSCs (IM-MSCs) to identify nuclei. Scale bar=25 mm. **(B)** Apoptotic index expressed as number of apoptotic myonuclei per 10^3 myofibers. * $p < 0.05$, vs. WB group; # $p < 0.05$, vs. IM-PBS group. The data presented are the mean \pm standard deviation.

inhibit muscle reconstruction, and injection of MSCs probably was performed too soon to modify atrophy, so more study on this topic is required.

Satellite cells are quiescent but poised for activation. Skeletal muscle regeneration mainly depends on satellite cells, and myonuclei loss might be replenished by activation and myogenic differentiation of satellite cells. Thus, satellite cells were assessed by Pax7, a transcription factor expressed when quiescent and proliferating [24]. We observed that the proliferative potential of satellite cells was impaired during immobilization because BrdU⁺/Pax7⁺ subpopulations were decreased in immobilized limbs. More BrdU⁺/Pax7⁺ subpopulations were present in the IM-MSC group compared with the IM-PBS group, which may suggest that MSCs contribute to satellite cell proliferation to some degree. The present study demonstrated that MSCs are not apparently attributable to differentiation into resident cell types, but rather to release of paracrine factors that improve cell microenvironments to make repairs [25]. In our study, we found no resident cells with GFP. Indeed, studies indicate that MSCs stimulate skeletal myoblast proliferation and differentiation via the release of paracrine factors such as S1P (sphingosine 1-phosphate) [26] or VEGF (vascular endothelial growth factor) [27].

Hind limb immobilization causes myonuclear apoptosis [28] and we observed more apoptotic myonuclei in the IM-PBS group

compared with the WB and IM-MSC groups. According to the myonuclei domain hypothesis, pro-apoptotic features are essential for increasing apoptotic myonuclei. Recent studies reported that the death receptor pathway and the mitochondrial pathway might be involved in regulating apoptosis. The mitochondrial pathway, in which Bax and Bcl-2 are important, plays a central role in triggering apoptosis [29]. Because limited evidence is available for death receptor pathway involvement in apoptosis induced by muscle wasting, such as immobilization and suspension, we concentrated on mitochondrial pathways. We noted more Bax expression and reduced Bcl-2 expression in the IM-PBS group. Therefore, the balance between Bax and Bcl-2 determines the onset of apoptosis, and differential expression of Bax and Bcl-2 protein indicate that immobilization can activate the mitochondrial apoptotic pathway. Simultaneously, the IM-MSC group had greater Bcl-2 protein expression and lower Bax protein expression than the IM-PBS group. TUNEL staining showed that MSCs significantly reduced apoptotic indices in the IM-MSC group compared with the IM-PBS group. These results suggest that MSCs rescued myonuclei from apoptosis, apparently by regulating the expression of Bcl-2 and Bax.

Akt is a serine/threonine kinase and a critical signaling component for regulating cellular metabolism, growth, and survival in multiple systems. In skeletal muscle, Akt phosphorylation activates protein synthesis to cause hypertrophy. Emerging

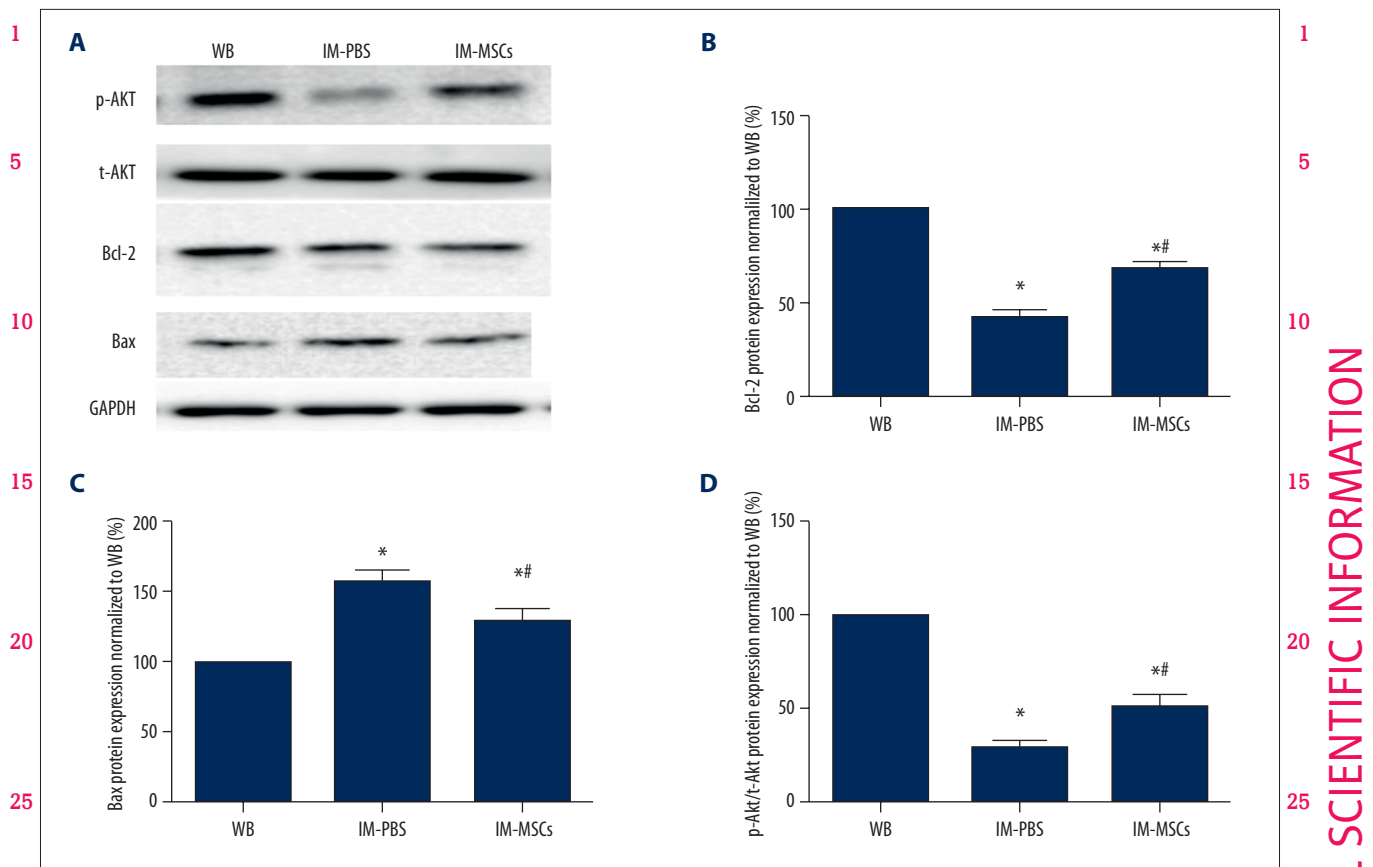


Figure 6. p-Akt, t-Akt, Bcl-2, and Bax were examined by Western blot analysis. (A) Representative blots for p-Akt, t-Akt, Bcl-2, and Bax expression in each group. (B) Bcl-2 protein expression normalized to WB group. (C) Bcl-2 protein expression normalized to WB group. (D) p-Akt/t-Akt protein expression normalized to WB group. * $p < 0.05$, vs. WB group; # $p < 0.05$, vs. IM-PBS group. The data presented are the mean \pm standard deviation.

evidence indicates that Akt may modulate cell proliferation and differentiation in diverse cell types. Activated Akt can induce subsequent phosphorylation of intracellular downstream factors such as mTOR. *In vitro* studies suggest that overexpression of mTOR induces differentiation of several cells types, such as osteoblasts, adipocytes, and neurons, as well as stimulating proliferating myoblast cells to differentiate and fuse into multinucleated myotubes. Because osteoblasts, adipocytes, and myocytes are derived from common precursor cells – MSCs – mTOR may determine lineage differentiation of these stem cells [30]. p-Akt/Akt ratios in the soleus muscle decreased after 14 d of immobilization in the IM-PBS group, but these ratios decreased after MSC treatment and BrdU⁺/Pax7⁺ cells increased. Thus, the Akt pathway may be activated by MSCs.

References:

- Grosset J-F, Onambele-Pearson G: Effect of foot and ankle immobilization on leg and thigh muscles' volume and morphology: A case study using magnetic resonance imaging. *Anat Rec (Hoboken)*, 2008; 291: 1673–83
- Metoki N, Sato Y, Satoh K et al: Muscular atrophy in the hemiplegic thigh in patients after stroke. *Am J Phys Med Rehabil*, 2003; 82: 862–65
- Thomas CK, Zaidner EY, Calancie B, Broton JG, Bigland-Ritchie BR: Muscle weakness, paralysis, and atrophy after human cervical spinal cord injury. *Exp Neurol*, 1997; 148: 414–23
- Adams GR, Caiizzo VJ, Baldwin KM: Skeletal muscle unweighting: Spaceflight and ground-based models. *J Appl Physiol*, 2003; 95: 2185–201

Conclusions

MSCs injected during hind limb immobilization maintain satellite cell pools and prevent apoptosis after atrophy. They may represent an adjunct intervention for controlling skeletal muscle protein synthesis and activation of satellite cells, even though soleus mass was not improved. The regulation of protein might be related to the Akt pathway. To demonstrate the dependent effects, more experiments are needed. Future studies should focus on muscle regenerative capacity and mass preservation.

- 1 5. Sato S, Ogura Y, Kumar A: TWEAK/Fn14 signaling axis mediates skeletal muscle atrophy and metabolic dysfunction. *Front Immunol*, 2014; 5: 18
6. Bodine SC, Stitt TN, Gonzalez M et al: Akt/mTOR pathway is a crucial regulator of skeletal muscle hypertrophy and can prevent muscle atrophy *in vivo*. *Nat Cell Biol*, 2001; 3: 1014–19
- 5 7. Rommel C, Bodine SC, Clarke BA et al: Mediation of IGF-1-induced skeletal myotube hypertrophy by PI(3)K/Akt/mTOR and PI(3)K/Akt/GSK3 pathways. *Nat Cell Biol*, 2001; 3: 1009–13
8. Chargé SBP, Rudnicki MA: Cellular and molecular regulation of muscle regeneration. *Physiol Rev*, 2004; 84: 209–38
9. Schultz E, McCormick K: Skeletal muscle satellite cells. *Rev Physiol Biochem Pharmacol*, 1994; 123: 213–57
- 10 10. Mitchell PO, Pavlath GK: Skeletal muscle atrophy leads to loss and dysfunction of muscle precursor cells. *Am J Physiol Cell Physiol*, 2004; 287: C1753–62
11. Grabowska I, Streminska W, Janczyk-Ilach K et al: Myogenic potential of mesenchymal stem cells – the case of adhesive fraction of human umbilical cord blood cells. *Curr Stem Cell Res Ther*, 2013; 8: 82–90
- 15 12. De Bari C, Dell'Accio F, Vandenabeele F et al: Skeletal muscle repair by adult human mesenchymal stem cells from synovial membrane. *J cell Biol*, 2003; 160: 909–18
13. von Roth P, Duda GN, Radojewski P et al: Mesenchymal stem cell therapy following muscle trauma leads to improved muscular regeneration in both male and female rats. *Gend Med*, 2012; 9: 129–36
- 20 14. Snijders T, Wall BT, Dirks ML et al: Muscle disuse atrophy is not accompanied by changes in skeletal muscle satellite cell content. *Clin Sci*, 2014; 126: 557–66
15. Shi D, Reinecke H, Murry CE, Torok-Storb B: Myogenic fusion of human bone marrow stromal cells, but not hematopoietic cells. *Blood*, 2004; 104: 290–94
- 25 16. Khan MA, Sahani N, Neville KA et al: Nonsurgically induced disuse muscle atrophy and neuromuscular dysfunction upregulates alpha7 acetylcholine receptors. *Can J Physiol Pharmacol*, 2013; 92: 1–8
17. Yeung EW, Head SI, Allen DG: Gadolinium reduces short-term stretch-induced muscle damage in isolated mdx mouse muscle fibres. *J Physiol*, 2003; 552: 449–58
18. Alway SE, Pereira SL, Edens NK et al: β -hydroxy- β -methylbutyrate (HMB) enhances the proliferation of satellite cells in fast muscles of aged rats during recovery from disuse atrophy. *Exp Gerontol*, 2013; 48: 973–84
19. Ninagawa NT, Isohe E, Hirayama Y et al: Transplanted mesenchymal stem cells derived from embryonic stem cells promote muscle regeneration and accelerate functional recovery of injured skeletal muscle. *Biores Open Access*, 2013; 2: 295–306
20. Joe AW, Yi L, Natarajan A et al: Muscle injury activates resident fibro/adipogenic progenitors that facilitate myogenesis. *Nat Cell Biol*, 2010; 12: 153–63
21. Kuraitis D, Giordano C, Ruel M et al: Exploiting extracellular matrix-stem cell interactions: A review of natural materials for therapeutic muscle regeneration. *Biomaterials*, 2012; 33: 428–43
22. Zhang B-T, Yeung SS, Liu Y et al: The effects of low frequency electrical stimulation on satellite cell activity in rat skeletal muscle during hindlimb suspension. *BMC Cell Biol*, 2010; 11: 87
23. Ohira T, Terada M, Kawano F et al: Region-specific responses of adductor longus muscle to gravitational load-dependent activity in Wistar Hannover rats. *PLoS One*, 2011; 6: e21044
24. Snijders T, Nederveen JP, McKay BR et al: Satellite cells in human skeletal muscle plasticity. *Front Physiol*, 2015; 6: 283
25. Sassoli C, Nosi D, Tani A et al: Defining the role of mesenchymal stromal cells on the regulation of matrix metalloproteinases in skeletal muscle cells. *Exp Cell Res*, 2014; 323: 297–313
26. Sassoli C, Frati A, Tani A et al: Mesenchymal stromal cell secreted sphingosine 1-phosphate (S1P) exerts a stimulatory effect on skeletal myoblast proliferation. *PLoS One*, 2014; 9: e108662
27. Sassoli C, Pini A, Chellini F et al: Bone marrow mesenchymal stromal cells stimulate skeletal myoblast proliferation through the paracrine release of VEGF. *PLoS One*, 2012; 7: e37512
28. Hao Y, Jackson JR, Wang Y et al: β -hydroxy- β -methylbutyrate reduces myonuclear apoptosis during recovery from hind limb suspension-induced muscle fiber atrophy in aged rats. *Am J Physiol Regul Integr Comp Physiol*, 2011; 301(3): R701–15
29. Jin Z, El-Deiry WS: Overview of cell death signaling pathways. *Cancer Biol Therapy*, 2005; 4: 147–71
30. Xiang X, Zhao J, Xu G et al: mTOR and the differentiation of mesenchymal stem cells. *Acta Biochim Biophys Sin (Shanghai)*, 2011; 43(7): 501–10
- 35 35. 35
- 40 40. 40
- 45 45. 45
- 50 50. 50
- 53 53. 53